# Longitudinal assessment of the neuroanatomical consequences of deep brain stimulation: Application of fornical DBS in an Alzheimer's mouse model

Daniel Gallino[a] *, Gabriel A. Devenyi[a,b], Jürgen Germann[a], Elisa Guma[c], Chloe Anastassiadis[c], M. Mallar Chakravarty[a,b,d] *

[a] Cerebral Imaging Center, Douglas Mental Health University Institute, Montreal Canada.
[b] Department of Psychiatry, McGill University, Montreal Canada.
[c] Integrated Program in Neuroscience, McGill University, Montreal Canada.
[d] Department of Biological and Biomedical Engineering, McGill University, Montreal Canada.

*corresponding authors (DG: dnlgallino@gmail.com; MMC: mallar@cobralab.ca)

Declarations of interest: none

**Keywords**

deep brain stimulation
DBS
fornix
longitudinal
MRI
mouse

## 1) Introduction

Deep brain stimulation (DBS) involves the delivery of electrical stimulation to dysfunctional brain circuits via surgically implanted leads containing electrodes. Current is then driven by programmable pulse generators which are permanently embedded in the patient, usually on the chest. Applying DBS to specific targets within the brain's motor circuitry has become the standard of care in the treatment of refractory movement disorders (Meidahl et al. 2017) , such as Parkinson's disease (Koller et al. 1997; Kumar et al. 1999) , dystonia (Vidailhet et al. 2005) and essential tremor (Blomstedt et al. 2007) . While such interventions have demonstrated consistent symptom improvement and management, the mechanisms behind the efficacy of DBS remain controversial, with evidence supporting DBS as both excitatory and inhibitory depending on context (Chiken and Nambu 2016).

The success observed in the treatment of movement disorders has sparked interest in investigating the use of DBS as a method of of treating other neuropsychiatric disorders (Sankar, Lipsman, and Lozano 2014). This interest, and an incidental finding during the use of DBS in treatment of morbid obesity (Hamani et al. 2008), led to the initiation of Phase I and II clinical trials examining the possibility of providing DBS to the fornix (DBS-f) as a possible treatment for Alzheimer's disease (AD) (Laxton et al. 2010; Lozano et al. 2016; Leoutsakos et al. 2018; Ponce et al. 2016). The fornix is a critical white matter pathway that integrates memory formation from the medial temporal lobe with rest of the cerebrum. As studies from the circuitry of Parkinson's disease have found, DBS produces downstream effects on signalling in connected structures (Hashimoto et al. 2003). It is therefore believed that by targeting the fornix, the broader circuitry of memory integration may be targeted with an end goal of improving memory and cognitive symptomatology of AD.

The results of these trials were mixed but encouraging, and demonstrated that while DBS-f did not reverse cognitive decline, it did seem to slow in older patients and transiently increased glucose metabolism in the temporal and parietal regions (Lozano et al. 2016)—the loss of which is considered a hallmark of AD (Mosconi 2005) . Furthermore, other studies from our group have demonstrated neuroanatomical remodelling throughout the brain and in the hippocampus specifically as a consequence of applying DBS-f (Sankar et al. 2015) and DBS to other neuroanatomical regions in the brains of mice (Chakravarty et al. 2016) (but see also (Sankar et al. 2016)) . These results are encouraging and demonstrate the potential of DBS-f to slow the neuroanatomical decline typically observed in AD. However, human AD DBS trials have been based on largely on the stimulation paradigms optimized for Parkinson's disease treatment that have already been approved by the FDA, i.e. chronic and high frequency (100 Hz and above). One of the proposed mechanisms of high frequency stimulation is the "depolarization blockade"; the rapid pace of delivery saturates the area with charge, preventing local neuron depolarization (Mogilner, Benabid, and Rezai 2001). If this is true, it is unclear that this chronic and high frequency strategy would be beneficial in treating AD, where an electrically generated lesion is not necessarily desired. The ability to model and test additional delivery regimes for DBS (chronic versus acute, frequency of stimulation, etc) in animal models using longitudinal study designs would be invaluable for further refinement of DBS or to examine novel targets such as the fornix.

Groups have observed improved memory in rat (Zhang et al. 2015) and mouse (Xia et al. 2017) models of AD after administering acute (24 and 1 hours respectively, both at 130 Hz and 90 μs pulses) DBS to another critical area of memory circuitry: the entorhinal cortex (EC), a critical region both in the context of AD and memory formation in general (Van Hoesen, Hyman, and Damasio 1991). Memory improvement was found at 3 weeks post-stimulation at earliest, suggesting the effects of DBS are not immediate. The timing of the initial emergence and the permanence of these effects is unknown as there are limited preclinical investigations of DBS in animal models that are performed with an intent to longitudinally monitor the progression of the disease and the impact that DBS may have on brain and behavioural phenotypes. In addition to scarce longitudinal data, many such studies omit female animals. Sex is believed to be a modulating factor in genetic risk for AD (Altmann et al. 2014; Damoiseaux et al. 2012) , as AD manifests with generally higher rates in females along with differences in disease progression, clinical profile, and susceptibility of risk factors (Mielke, Vemuri, and Rocca 2014) . While proof of principle for targeting memory-associated structures with DBS in AD animal models has been established, there remains much unexplored territory.

Here, we have used custom constructed magnetic resonance imaging (MRI)-compatible DBS electrodes that do not produce susceptibility artefacts that are commonly observed in the use of metallic electrodes. This experimental innovation allowed us to investigate neuroanatomical remodelling and memory function in relation to DBS-f in both sexes of a murine model of AD (3xTg) using longitudinal assessments of neuroanatomy (via structural MRI) and an adapted Morris water maze test (MWM). We provide details not only of our experiment but also of our electrode fabrication to enable future investigators to use this type of electrode design. The work presented here follows recent work from our group examining the impact of acute DBS on neuroanatomy (Chakravarty et al. 2016) and longitudinal phenotyping of animal models using structural MRI and behavioural assays (Kong et al. 2018).

## 2) Results

### 2.1) DBS effects on learning

#### 2.1.1) DBS improves performance of electrode implanted mice at 3 weeks post stimulation

The first trial of each water maze time point was excluded from learning measures as mice are naive to the platform's new location. The Cox proportional hazard model revealed a significant difference between stimulated (stim) and sham stimulated (sham) animals ($\alpha = 0.05$, $p < 0.0071$) 3 weeks after stimulation (fig. 3), with stimulated mice outperforming the sham group. Neither group was significantly different than skull hole controls which performed intermediately to stim and sham groups. Six weeks after stimulation, stim again outperformed the sham group as did the electrodeless group, but not significantly after multiple comparison correction ($p = 0.028$). The interaction term was not significant at other timepoints. See supplementary fig. S3 for all water maze time points. No significant differences were observed in thigmotaxis (circling the pool wall) or in initial heading error.

#### 2.1.2) DBS performance improvement is driven by males

Investigation of sex differences by Cox proportional hazard modeling revealed significant sex by treatment interactions at 3 and 6 weeks post-stimulation ($\alpha = 0.05$, $p < 0.0071$). Specifically, stimulation did not affect female performance significantly, but greatly improved that of males. Sham males performed poorly relative to all other treatment/sex combinations on these days. Stimulated males by contrast, reached and/or surpassed the performance level of other groups (fig. 4). The interaction term was not significant at other timepoints. See supplementary fig. S4 for all water maze time points. Once again, no significant differences were observed in thigmotaxis or in initial heading error.

## 2.2) DBS effects on long term memory

Overall, acute DBS-f did not produce significant lasting changes in long term memory, as approximated by the time-of-return to the previous week's platform position. Given the sex differences seen in learning, we chose to perform a post-hoc investigation of sex differences on longer term memory. Indeed, stimulated males showed significant improvement over their sham counterparts ($p < 0.05$) on week 4's pseudo probe trial of week 3's location in terms of mean latency to escape (fig. 5). Also similarly to learning measures, stimulated animals did not perform significantly better than skull hole controls.

## 2.3) Volumetric Effects of DBS

### 2.3.1) General Volumetric Effects

Voxel-based deformation analysis revealed a time point by treatment interaction; stimulated mice experienced different volumetric changes from their sham counterparts in diverse areas of the brain (fig. 6) (see supplementary fig. S5 for whole brain). By the final MRI time point, stimulated mice had accrued larger local volumes than the sham group in a region of the R superior colliculus ($q < 0.05$), L dorsal subiculum ($q < 0.15$), R posterior thalamus ($q < 0.15$) and R cerebral peduncle ($q < 0.15$). Conversely, stimulated mice had smaller volumes in the R central nucleus of the inferior colliculus ($q < 0.05$), dorsal medial periaqueductal gray ($q < 0.10$), R cingulate cortex areas 24 & 32 ($q < 0.10$) and L fimbria ($q < 0.10$) amongst others (see supplementary table S2 for full list).

### 2.3.2) Sex-Specific Volumetric Effects of DBS

As sex differences were prominent in behavioural outcomes, we chose to investigate if this was also the case for the volumetric effects of DBS. The linear mixed effects model revealed a sex by treatment by time point interactions across the brain, indicating that changes in volume due to stimulation by the final time point were modulated by sex (fig. 7, see supplementary fig. S6 for whole brain, supplementary table S3 for statistics). The areas whose volumes were affected by this sex interaction were far more widespread than the areas affected commonly by stimulation. The most widespread effects were observed bilaterally in cingulate cortex areas 24b & 32 ($q < 0.10$), along with the primary and secondary motor cortices ($q < 0.10$), where stimulation induced higher final volumes in males and lower final volumes in females. In contrast, a large

stretch of fimbria, alveus and external capsule ($q < 0.10$) bridging the more anterior auditory cortices and posterior visual cortices displayed the opposite relationship, in which stimulation resulted in higher final volumes for females, and lower volumes for males. Some areas, such as the gigantocellular reticular nucleus ($q < 0.10$), were nearly unaffected in one sex (males) while experiencing much more pronounced treatment differences in the other (stimulated females larger final volumes than sham counterparts).

**3) Discussion**

We endeavoured to design an experiment capable of capturing and evaluating the longitudinal effects of acute DBS-f in an Alzheimer's mouse model with measures of memory and brain imaging. Using custom-built carbon fiber electrodes, we delivered one hour of high frequency stimulation and followed the mice for a month and a half with a specialized weekly Morris water maze. MR images were taken before stimulation, soon after, and at the culmination of the experiment to evaluate volumetric changes.

Differences in failure rate and latency to platform between actively stimulated and sham stimulated groups emerged at 3 weeks post stimulation, with the next largest differences seen at 6 weeks. In both cases, stimulated males outperformed their sham counterparts in learning platform location. This sex-specific improvement in learning appeared to translate to superior recall one week later as stimulated males returned to the old platform location faster than the sham group. These results suggest that any lasting impact that DBS-f may have occurs in a localized period subsequent to DBS-f administration. Our behavioural results mirror cross-sectional findings in which AD mouse-models were subjected to acute, 1 hour DBS of the entorhinal cortex which improved fear context dependant memory 3 and 6 weeks later, although not 1 week later. Spatial memory as measured by the Morris water maze was also improved 6 weeks later, however the non-repeatability of the test limited the authors to that sole time point (Xia et al. 2017) . Our water maze design allowed a higher resolution determination of the timing of these effects.

We unexpectedly found sex to be a major mediating factor in water maze measures, with significant differences driven mostly by males. Females tended to perform well regardless of stimulation status. Sham stimulated males however, tended to be poorer performers, and could only perform as well as females once stimulated. Performance differences on cognitive tests have been known to differ significantly between the sexes in the progression of human AD. In mildly impaired patients with similar levels of hippocampal atrophy, others have found that females outperform males on verbal memory tasks, despite no difference seen in controls or fully progressed AD cases (Sundermann et al. 2016). Given the male sham stimulated group's poor performance relative to the male electrodeless controls, it is quite possible that the presence of the electrodes inadvertently was responsible for a difference in performance. Why this difference was not seen immediately after surgery, consistently after its appearance and only in males warrants further investigation. Interestingly, electrode presence in sham stimulated mice has previously been shown to increase astrocyte density, an effect which is not apparent when stimulation is actually applied (Chakravarty et al. 2016). Interestingly, others have found improvements in performance in non-AD, wild type mice at the 6 week mark post-DBS, a time where newly formed neurons that go on to form functional brain circuits in the dentate gyrus

have previously been observed (Stone et al. 2011) . While investigating effects on wild type mice fell outside the scope of our current research, there is no reason why future investigations should be limited to disease models. These results call into question whether current treatment paradigms which are based on the chronic stimulation regime used in Parkinson's patients (Koller et al. 1997), are necessarily the best approach to attempting to treat AD with DBS in humans. Other stimulation parameters, such as frequency, amplitude and second-level patterning such burst or pulse-train delivery, may also affect outcomes and will require investigation and optimization.

One hour alone of high frequency DBS delivered proximal to the fornix caused differences in local volumes of diverse areas of the brain, differences that seemed to persist for at least 45 days. Final group volume differences surpassed 20% change relative to baseline in some cases, with both higher and lower volumes seen as a result of stimulation. Some areas of change were common to both sexes while others depended highly on sex. Structures connected to or associated with the fornix in the Papez circuit (medial-limbic circuit), such as the subiculum of the hippocampus, the cingulate cortex, anterior thalamus and fimbria experienced volumetric changes, but were by no means over-represented or even necessarily the most affected. The greatest changes were found in the colliculi. These changes were unexpected, as these areas are not part the circuit of Papez and are associated with visual and auditory processing respectively. It is possible that differences in visual/auditory processing and coordinated movements could affect latencies, even though the morris water maze is primarily considered a test of memory.

While the exact mechanism of DBS in causing volumetric changes remains controversial, cellular changes caused by DBS such as the proliferation of dentate gyrus granule cells in rat hippocampi after high frequency stimulation of the anterior thalamus have been found (Hamani et al. 2011). The hypothesis that DBS acts through neurogenesis and/or the modulation of plasticity factors continues to gain ground as recent studies have found changes to expression, splicing, methylation and overall protein levels of genes involved in these processes (Pohodich et al. 2018), even in wild type mice receiving fornical stimulation. Furthermore, stimulation of the ventromedial prefrontal cortex of mice has been shown to increase blood vessel size and synaptic density in the hippocampus (Chakravarty et al. 2016). Stimulation of the nucleus basalis of Meynert in Alzheimer's mouse models has been shown to downregulate apoptotic genes and improve cellular survival in the hippocampus along with improving water maze performance (Huang et al. 2019). Given that both increases and decreases are observed in this work along with differing trajectories, it seems reasonable to conclude that a variety of different processes may contribute to this remodelling. As for sex differences in volume effects, white matter developmental trajectories and organization are also known to be sex-specific in humans and believed to be influenced by hormonal profiles (Perrin et al. 2008; Kaczkurkin, Raznahan, and Satterthwaite 2018). It is therefore not surprising that the most pronounced areas of sex difference found were located in white matter areas. The pronounced sex differences found underscore the importance of conducting trials with both sexes. It is very often the case that females are excluded entirely from preclinical experiments due to concerns that female hormone cycling will introduce variance (Qiu et al. 2013). This disincentive to include females can lead to false conclusions about the effectiveness, safety and significantly limit generalizability of treatments under investigation in preclinical trials particularly in light of recent work on the pronounced sex-differences in normative mouse brain anatomy (Qiu et al. 2018).

It should be noted that a limitation of behavioural assay was that the weekly task difficulty in the water maze could not be held exactly the same. Platform-wall distance had to be varied to stop mice from memorizing that distance and merely swimming in circles to locate the platform on new days. This meant that the distance from the start location to the goal (and therefore difficulty) could not be held constant. Performance measures can only fairly be compared within day, and not across days. It could be that stimulation effects are present on other days, but treatment groups are only sufficiently challenged on certain days to capture this difference.

Next, for the MRI assay, while manganese served as an effective contrast enhancement agent, it is also a known neurotoxin. While it is well established in rodent MRI literature, and used in doses believed to not to inhibit spatial learning (Vousden et al. 2018), others have shown chronic exposure to lead to Parkinson's like symptoms in mice, when given 30 mg/kg daily for three weeks (Sepúlveda et al. 2012). Given that we feel the experiment would be improved with more imaging at the behavioural times of interest we identified, cumulative dose can become an issue. In addition to this, there would be concern that such frequent use of anaesthetics might interfere with behavioural memory tasks, or with anatomical features. For these reasons, we choose to limit MRI acquisitions to a baseline, proximal and long-term measurement.

Using a DBS system with carbon-based electrodes for mice did not allow for a completely faithful recreation of human conditions. Normally pulse generators are implanted within the patient and act as a return electrode for the DBS circuit. However, at dimensions of 3 by 3 by 5 cm, pulse generators had to be kept exterior to the mice due to their sheer size. Our attempts to use the tail, skin or skull as the point of contact for the return resulted in a high resistance which would have required a dangerous amount of voltage to drive the current. We therefore opted to place the return electrode in the brain itself. As the return electrode would also produce an electric field (albeit opposite to the anode) which could cause off-target effects if placed anywhere else, we settled on placing the return symmetrically across from the anode.

## 4) Conclusions

We have developed a experimental template for following DBS events in a longitudinal fashion that can yield a timeline of phenotypic effects in terms of both behaviour and imaging. We have found evidence that the effects of DBS-f emerge in a chronological and sex specific manner, with effects presenting mostly in males at 3 and 6 weeks post-stimulation. This required only an hour of high frequency DBS-f as opposed to chronic regimens trialed in humans. Acute stimulation affected local volume trajectories in diverse areas of the brain, with both increases and decreases seen relative to controls. While volumetric remodelling occured in both sexes, its effects were rarely co-localized. The non-uniformity of these trajectories hints that different underlying processes are contributing to these changes, which warrant further investigation. Deep brain stimulation holds promise as a future treatment for Alzheimer's disease, and longitudinal studies that chronicle both anatomical and behavioural changes with high resolution have much to contribute to the preclinical investigation of optimal treatment strategies.

## 5) Methods and Materials

5.1) Animals

The Toronto Triple Transgenic (3xTg) mice ( B6;129-Psen1Tg[APPSwe,tauP301L]1Lfa/Mmjax) harbours 3 mutations typically associated with familial variants of AD (Oddo et al. 2003) . The APP KM670/671NL (Swedish) is a double point mutation which increases overall Aβ production (Citron et al. 1992) and is associated with abnormal memory decline in humans (Mullan et al. 1992) . The MAPT P301L mutation affects the microtubule stabilizing protein tau, which leads to neurofibrillary tangles (Hutton et al. 1998) . Finally, the presenilin mutation PSEN1 M146V affects the activity of the gamma secretase complex which cleaves APP, and is also associated with familial dementia (Riudavets et al. 2013) . It is important to note that mouse models such as the 3xTg are dependant on genetic manipulation to produce consistent AD-like symptoms and as such, are expected to be more representative of genetically-driven, familial forms of AD. 3xTg mice experience cognitive impairment manifest as memory deficits in water maze beginning at 4 months along with increased intracellular Aβ, plaque deposition at 6 months and finally tau pathology by a year of age (Billings et al. 2005) . This line and its 4 month start of water maze memory impairment has been longitudinally phenotyped previously by our group using behavioural and MRI assays (Kong et al. 2018; Rollins et al., n.d.). Early impairment (at 4 months) seems to be specific to spatial memory, while other types such as recognition tend to be impaired later (at 9 months) (Clinton et al. 2007). Both sexes of mice were included in all experiments. Animals were all hemizygous, born of 3xTg fathers and C57Bl/6 mothers. 8-9 mice of each sex were assigned pseudo-randomly to stimulation (n = 17, m/f = 9/8), sham stimulation (n = 17, m/f = 8/9) or electrodeless control groups (n = 16, m/f = 8/8).

All animal experiments were approved by the McGill University Animal Care Committee and carried out in compliance with both the Canadian Council on Animal Care guidelines. Mice were kept in standard housing conditions with food and water ad libitum. The light cycle consisted of 12 hours on during the day (8am to 8pm), 12 hours off during the night, with all manipulations and assays performed during daytime. Experimental animals were bred in-facility to avoid confounds from the stress of transportation, then weaned at postnatal day (PND) 21 into cages of up to 5 siblings, separated by sex.

5.2) Experimental Outline

At 2 months of age, (1st week of experiment) mice received 3, 10 min handling sessions over 3 days to acclimate them to experimenter manipulation. During the week 2 of the experiment, mice received 5 days of water maze training. Surgeries for electrode implantation (fabrication details below) were performed at week 3 of the experiment. Mice were given 2 weeks to recover from surgical procedures before receiving DBS, sham DBS or no treatment in the case of no-electrode controls. MRIs were acquired 4 days before stimulation (baseline), 3 days after, and 6 weeks after stimulation for follow-up. Throughout the experiment, mice were assessed with a weekly Morris water maze where platform location was varied to limit impact of habituation, including one preoperative time point, one post-operative but pre-stimulation time point and 7 post-stimulation time points. Overall, this timeline was chosen with the intention of intervening with DBS before cognitive decline begins, with follow-up extending into the prodromal stage. See fig. 1 for timeline.

5.3) Electrode Design and Components

Carbon fibre was chosen for electrode construction due to its conductive properties, biocompatibility and to better mimic the magnetic properties of brain tissue as opposed to metals such as stainless steel (Chakravarty et al. 2016). Each electrode consisted of two carbon fibre rods (goodwinds.com, Mount Vernon, WA USA, # CS010048, CS080048), a transcranial rod (diameter 0.25 mm, length 8 mm) and an extracranial rod (diameter 2 mm, length 5 mm) annealed together with conductive carbon epoxy (Atom Adhesives, Fort Lauderdale FL, USA, # AA-CARB 61) in parallel fashion and insulated with spray-on rubber (Plasti Dip multipurpose coating) (Performix, Blaine MN, USA, #11203). The transcranial rod protruded 3 mm into the skull, where the uninsulated end (simple cross sectional area of rod) made contact with tissue. The thicker, extracranial rod served both as an anchor to attach the electrode to the skull and as an attachment point for wiring (fig. 2). See supplementary methods for construction details.

5.4) Stereotaxic Surgeries

Mice were anaesthetized with isoflurane (5% induction, ~1.5% maintenance), given an injection with 20 mg/kg carprofen for future pain relief and positioned into a stereotaxic platform. Half-millimetre diameter holes were drilled into the skull bilaterally (+/- 0.75 mm) at bregma anterior/posterior-wise. George Paxinos and Keith B.J. Franklin's "The Mouse Brain In Stereotaxic Coordinates" Fourth Edition atlas was used to identify coordinates for targeting the fornix. In DBS or sham DBS bound groups, the custom-built carbon electrodes were inserted at a depth of 3 mm, placing them on either side of, but without damaging, the anterior limbs of the fornices (fig. 2). This mimics the surgical implantation technique where electrodes were placed tangential to the fornices without puncturing them (Ponce et al. 2016; Lozano et al. 2016). The left electrode serves as an anode and the right as cathode in stimulation. Animals in the no-electrode group merely had holes drilled while maintaining all other surgical conditions. The electrodes were secured to the skull with a thin layer of quick-drying glue (Krazy Glue, High Point NC, USA, # KG582) and allowed 3 min to dry. For structural stability, a 2-3 mm high mound of dental cement (Parkell, Edgewood NY, USA, # S380) was then applied and allowed 5 min to dry in order to secure the base of the electrodes and finish sealing the wound. A typical surgery lasted approximately 40 min. Over the course of the experiment, 2 mice lost their electrodes and were removed from the experiment.

5.5) Stimulation

Mice were anaesthetized with 5% isoflurane briefly while wires from a custom-built pulse generator and accompanying programming software (Rogue Research Inc., Montreal QC, Canada) were attached to their electrodes. Once recovered, the mice were allowed to move freely around an open cage for the duration of stimulation or sham stimulation (supplementary fig. S1). The no-electrode group was not manipulated. A high-frequency electrical paradigm was chosen to reflect previous work in fornical stimulation of rodents (Hescham et al. 2013). Monophasic DBS was delivered at 100 Hz, with a pulse width of 100 μs, adjusting voltage to drive 100 μA of current (subject to differing resistivity for each mouse, but generally requiring approximately 3 V). Stimulation and sham stimulation (connected to the pulse generator but no stimulation) lasted 1 hour.

5.6) Morris water maze

This experiment differed from traditional water maze designs (Vorhees and Williams 2006) as a longitudinal, platform-switching method—also known as matching-to-sample)—was used in both training and evaluation time points. Traditional designs train mice heavily for an entire week to memorize the hidden location of an escape platform. The platform is then removed, and the amount of time the animal spends in proximity to its former location is gauged (known as a probe trial) to assess memory. This test is seldom repeated in a longitudinal fashion to track how memory capabilities change, because any subsequent evaluation of performance would be unable to distinguish between animals residing in the platform location due to recent training or due to longer term memories formed from previous evaluations. In order to continuously evaluate learning and memory with high temporal resolution, we therefore used a matching-to-sample paradigm similar to that used in (Williams et al. 2003), but with some modifications. We found in our pilot studies that the 3xTg mice were poorer learners than the rats for which the method was originally designed for, thus 4 trials per day were given to demonstrate learning instead of 2. Mice were also poorer at reversal learning and displayed strong, persistent biases throughout all 4 trials for previous platform locations when tested on back-to-back days. Testing was moved to a weekly basis as a compromise between detecting biases for previous platform locations (now only seen on the first, naive trial if at all) while not greatly interfering with the acquisition of the new location.

Each evaluation day for the animals started with them being naive to the new location of the platform. We took advantage of this naivety to observe if the mice carried forward any preference for the last week's platform location as an assessment of long-term memory. We refer to this first, naive trial as a "pseudo probe trial" (pseudo because the platform has been removed from the old location like a conventional probe trial, but has not been removed from the pool entirely and is merely at new location). It should be stressed that the pseudo probe trial is not equivalent to conventional probe trials due to 1) the possibility of the trial being prematurely terminated by an accidental finding of the new platform, 2) mice receive a single day of training as opposed to a week's worth and 3) the trial is conducted a full week after the training as opposed to the next day. This design also allowed us to assess shorter-term memory formation (which we will refer to as "learning"), on a weekly basis. This was measured by the success rate of finding the platform as well as the reduction in time required to do so on non-naive trials.

The pool was 1.5 m in diameter, kept at 21°C, with water made opaque with white tempera paint. Visual cues included 3 distinct black and white symbols, approx 10 cm in diameter at N, SW and E directions (supplementary fig. S2). Mice were assessed during their day cycle, at a light level of 20 lumen. Each weekly assessment day, the mice were given 4 trials of 120 s to attempt to find a 9 cm diameter platform hidden 1.5 cm below the surface of the pool. If a mouse failed to find the platform within that time, it was guided to the location by hand. Upon reaching the platform, mice were given 15 s to learn their surroundings before being rescued. The task is extremely challenging by design, which we hoped would allow us to capture subtle differences between treatment groups. Our previous experience characterizing the 3xTg line in a conventional water maze informed our choices for ensuring this level of challenge; a larger pool size (up from 1.2 m diameter), a smaller platform (down from a width of 15 cm) and an

increased trial time (from 60 s) (Kong et al. 2018). On successive days, the location of the platform was changed to a different location based on both quadrant and distance-to-centre (supplementary table S1). To acclimatize the mice to the maze and task, the experiment began with an initial training period, consisting of 5 such days contiguously (see fig. 1). Preoperative, and postoperative assessments were used to gauge if or how performance was affected by surgery itself.

5.7) MRI

24 hours before undergoing each MRI, mice were injected with 62.5 mg/kg of manganese chloride ($MnCl_2$) for the purposes of contrast enhancement. Injections were initially subcutaneous, but after several adverse skin reactions (a problem others have experienced with this administration route (Vousden et al. 2018)), they were replaced by the intraperitoneal route. To account for any potential resulting differences in behaviour or anatomy, cohort was included as a random effect in statistical modelling.

Injections $Mn^{2+}$ ions "mimic" $Ca^{2+}$ and are preferentially taken up in certain brain structures (such as CA3 of the hippocampus), by voltage-gated calcium channels (Lin and Koretsky 1997) which shortens the T1 relaxation time (Lauterbur 1973) of those structures and to a degree, the brain in general, allowing for better contrast (Aoki et al. 2004). During imaging, mice were anaesthetized with 1.5% isoflurane in oxygen. Imaging was conducted in a Bruker 7T, 30 cm bore magnet with AVANCE electronics. A 3D FLASH (Fast, Low Angle SHot) sequence previous used by our group (Kong et al. 2018) was used with TE/TR of 4.5 ms / 20 ms, flip angle of 20° and zero-fill acceleration factor of 1.34, generating 100 μm isotropic images (matrix size of 180 x 160 x 90) in 14.5 min with 2 averages. Images were assessed for motion and electrode artifacts, and to confirm electrode targeting. Although no electrode artifacts were visually detectable, subsequent interpretation of deformation results disregarded results found within 3 voxels of the electrodes as a precaution. Electrodes were considered mistargeted when any exposed lead deviated more than 0.3 mm from target coordinates.

5.8) Image Processing

Images were exported as DICOM files (Digital Imaging and COmmunications in Medicine) and converted to MINC format (Medical Imaging Net CDF) (Vincent et al. 2016). In preprocessing, images were stripped of their native coordinate system, left-right flipped to compensate for Bruker's native radiological coordinate system, denoised using patch-based adaptive non-local means algorithm (Coupe et al. 2008), and affinely registered to an average mouse template to produce a rough brain mask. The images were then corrected for inhomogeneity using N4ITK (Tustison et al. 2010) at a minimum distance of 5 mm. Finally, a descaled/desheared version of the affine registration was used to apply a grid-preserving, rigid resample to the corrected scan into the mouse template space. The denoised and inhomogeneity-corrected images were then used as input for the 2 level model building image registration tool component of the Pydpiper toolkit (Friedel et al. 2014) . Image registration occurs in two steps: using a within subject registration followed by a group-wise registration strategy. For within subject registration, a subject specific model is created by performing rigid, affine and finally iterative nonlinear registration that creates an average representation of a specific subjects anatomy over the course

of the experiment using a hierarchical multi-resolution registration strategy (Avants, Tustison, and Song 2009). Once these averages are created, they are used as inputs towards the construction of a group average which is used to create a common space that allows for group-level, longitudinal comparisons (Kong et al. 2018). Nonlinear transformations are then concatenated and the log-transformed Jacobian determinants are estimated (Chung et al. 2003) and are used to reflect relative volume change at the subject level over time. As the electrodes introduced differences in local brain shape, electrodeless controls were not included in this analysis so as to not introduce known structural confounders. Jacobian determinants were log transformed and blurred at 0.2 mm full-width, half-maximum to better conform to Gaussian assumptions for statistical testing.

5.9) Statistics

Statistical analysis was performed in R (R Core Team 2016) (programming language and software environment for statistics), and image analysis was performed using the (Lerch et al. 2016). Latency and failure rates in water maze were modelled using a Cox Proportional Hazard model (Kassambara et al. 2018). This cumulative incidence model is considered superior to the t-test or ANOVA often used in water maze analysis because allows for 1) non-parametrically distributed latency times 2) the unbiased inclusion of failures (trials where mice do not find the platform within the time limit is usually excluded or counted as a max time value) and 3) the ability to include covariates and test for their explanatory contributions (Jahn-Eimermacher, Lasarzik, and Raber 2011).

Our general Cox model tested the ability of treatment group to explain the rates of successfully finding the platform in the water maze over time, along with cohort and trial number as covariates.

Bonferroni correction was applied to account for multiple comparisons across testing days. A second Cox model tested the ability of ability of a treatment group by sex interaction to explain the rates of successfully finding the platform in the water maze over time, along with cohort and trial number as covariates. Bonferroni correction was also applied here to account for multiple days (7) being tested.

The non-parametric Mann-Whitney *U* test was used to evaluate differences in pseudo-probe trials of previous platform recall due to multiple failure criteria being present (mice can “fail” to return to due to both finding the new platform first or timing out).

Relative Jacobian outputs from Pydpiper were modelled with a linear mixed-effects models. In the general model, Jacobians were predicted by a time point (as factor, comparison to baseline) by treatment interaction with cohort and subject included as random effects. The sex specific model was identical, excepting that sex was added to the interaction term.

The FDR (False Discovery Rate) correction method (Benjamini and Hochberg 1995) was used to correct for multiple comparisons across voxels.

**Author Contribution Statement:** DG and MMC designed the study. DG performed the imaging, took behavioural measures conducted analyses, wrote the main manuscript text and prepared figures and tables. GD and JG provided scientific and extensive computational consultation. EG and CA provided coding framework used in analysis. All authors reviewed the manuscript and MMC supervised the project.

**Acknowledgements:** This work was made possible by contributions from the Brain Canada Foundation, the Natural Sciences and Engineering Research Council (NSERC), the Canadian Institutes of Health Research (CIHR) and the Fonds de Recherche du Québec - Santé (FRQS). Funding sources played no part in the design of the study. We would also like to thank Dr. Stephen Frey and the development team at Rogue Research for their help customizing the construction and programming of the pulse generators.

**Data Availability Statement:** The datasets generated during and/or analysed during the current study are available from the corresponding author on reasonable request.

## References

Altmann, Andre, Lu Tian, Victor W. Henderson, Michael D. Greicius, and Alzheimer's Disease Neuroimaging Initiative Investigators. 2014. "Sex Modifies the APOE-Related Risk of Developing Alzheimer Disease." *Annals of Neurology* 75 (4): 563–73.

Aoki, Ichio, Yi-Jen Lin Wu, Afonso C. Silva, Ronald M. Lynch, and Alan P. Koretsky. 2004. "In Vivo Detection of Neuroarchitecture in the Rodent Brain Using Manganese-Enhanced MRI." *NeuroImage* 22 (3): 1046–59.

Avants, Brian B., Nick Tustison, and Gang Song. 2009. "Advanced Normalization Tools (ANTS)." *The Insight Journal* 2: 1–35.

Benjamini, Yoav, and Yosef Hochberg. 1995. "Controlling the False Discovery Rate: A Practical and Powerful Approach to Multiple Testing." *Journal of the Royal Statistical Society. Series B, Statistical Methodology* 57 (1): 289–300.

Billings, Lauren M., Salvatore Oddo, Kim N. Green, James L. McGaugh, and Frank M. LaFerla. 2005. "Intraneuronal Abeta Causes the Onset of Early Alzheimer's Disease-Related Cognitive Deficits in Transgenic Mice." *Neuron* 45 (5): 675–88.

Blomstedt, P., G-M Hariz, M. I. Hariz, and L-O D. Koskinen. 2007. "Thalamic Deep Brain Stimulation in the Treatment of Essential Tremor: A Long-Term Follow-Up." *British Journal of Neurosurgery* 21 (5): 504–9.

Chakravarty, M. Mallar, Clement Hamani, Alonso Martinez-Canabal, Jacob Ellegood, Christine Laliberté, José N. Nobrega, Tejas Sankar, Andres M. Lozano, Paul W. Frankland, and Jason P. Lerch. 2016. "Deep Brain Stimulation of the Ventromedial Prefrontal Cortex Causes Reorganization of Neuronal Processes and Vasculature." *NeuroImage* 125 (January): 422–27.

Chiken, Satomi, and Atsushi Nambu. 2016. "Mechanism of Deep Brain Stimulation: Inhibition, Excitation, or Disruption?" *The Neuroscientist: A Review Journal Bringing Neurobiology, Neurology and Psychiatry* 22 (3): 313–22.

Chung, Moo K., Keith J. Worsley, Steve Robbins, Tomás Paus, Jonathan Taylor, Jay N. Giedd, Judith L. Rapoport, and Alan C. Evans. 2003. "Deformation-Based Surface Morphometry Applied to Gray Matter Deformation." *NeuroImage* 18 (2): 198–213.

Citron, M., T. Oltersdorf, C. Haass, L. McConlogue, A. Y. Hung, P. Seubert, C. Vigo-Pelfrey, I.

Lieberburg, and D. J. Selkoe. 1992. “Mutation of the Beta-Amyloid Precursor Protein in Familial Alzheimer’s Disease Increases Beta-Protein Production.” *Nature* 360 (6405): 672–74.

Clinton, Lani K., Lauren M. Billings, Kim N. Green, Antonella Caccamo, Jerry Ngo, Salvatore Oddo, James L. McGaugh, and Frank M. LaFerla. 2007. “Age-Dependent Sexual Dimorphism in Cognition and Stress Response in the 3xTg-AD Mice.” *Neurobiology of Disease* 28 (1): 76–82.

Coupe, P., P. Yger, S. Prima, P. Hellier, C. Kervrann, and C. Barillot. 2008. “An Optimized Blockwise Nonlocal Means Denoising Filter for 3-D Magnetic Resonance Images.” *IEEE Transactions on Medical Imaging* 27 (4): 425–41.

Damoiseaux, Jessica S., William W. Seeley, Juan Zhou, William R. Shirer, Giovanni Coppola, Anna Karydas, Howard J. Rosen, et al. 2012. “Gender Modulates the APOE ε4 Effect in Healthy Older Adults: Convergent Evidence from Functional Brain Connectivity and Spinal Fluid Tau Levels.” *The Journal of Neuroscience: The Official Journal of the Society for Neuroscience* 32 (24): 8254–62.

Friedel, Miriam, Matthijs C. van Eede, Jon Pipitone, M. Mallar Chakravarty, and Jason P. Lerch. 2014. “Pydpiper: A Flexible Toolkit for Constructing Novel Registration Pipelines.” *Frontiers in Neuroinformatics* 8 (July): 67.

Hamani, Clement, Mary Pat McAndrews, Melanie Cohn, Michael Oh, Dominik Zumsteg, Colin M. Shapiro, Richard A. Wennberg, and Andres M. Lozano. 2008. “Memory Enhancement Induced by Hypothalamic/fornix Deep Brain Stimulation.” *Annals of Neurology* 63 (1): 119–23.

Hamani, Clement, Scellig S. Stone, Ariel Garten, Andres M. Lozano, and Gordon Winocur. 2011. “Memory Rescue and Enhanced Neurogenesis Following Electrical Stimulation of the Anterior Thalamus in Rats Treated with Corticosterone.” *Experimental Neurology* 232 (1): 100–104.

Hashimoto, Takao, Christopher M. Elder, Michael S. Okun, Susan K. Patrick, and Jerrold L. Vitek. 2003. “Stimulation of the Subthalamic Nucleus Changes the Firing Pattern of Pallidal Neurons.” *The Journal of Neuroscience: The Official Journal of the Society for Neuroscience* 23 (5): 1916–23.

Hescham, Sarah, Lee Wei Lim, Ali Jahanshahi, Harry W. M. Steinbusch, Jos Prickaerts, Arjan Blokland, and Yasin Temel. 2013. “Deep Brain Stimulation of the Forniceal Area Enhances Memory Functions in Experimental Dementia: The Role of Stimulation Parameters.” *Brain Stimulation* 6 (1): 72–77.

Huang, Chuyi, Heling Chu, Yu Ma, Zaiying Zhou, Chuanfu Dai, Xiaowen Huang, Liang Fang, Qiang Ao, and Dongya Huang. 2019. “The Neuroprotective Effect of Deep Brain Stimulation at Nucleus Basalis of Meynert in Transgenic Mice with Alzheimer’s Disease.” *Brain Stimulation* 12 (1): 161–74.

Hutton, M., C. L. Lendon, P. Rizzu, M. Baker, S. Froelich, H. Houlden, S. Pickering-Brown, et al. 1998. “Association of Missense and 5’-Splice-Site Mutations in Tau with the Inherited Dementia FTDP-17.” *Nature* 393 (6686): 702–5.

Jahn-Eimermacher, Antje, Irina Lasarzik, and Jacob Raber. 2011. “Statistical Analysis of Latency Outcomes in Behavioral Experiments.” *Behavioural Brain Research* 221 (1): 271–75.

Kaczkurkin, Antonia N., Armin Raznahan, and Theodore D. Satterthwaite. 2018. “Sex Differences in the Developing Brain: Insights from Multimodal Neuroimaging.”

*Neuropsychopharmacology: Official Publication of the American College of Neuropsychopharmacology*, June. https://doi.org/10.1038/s41386-018-0111-z.

Kassambara, Alboukadel, Marcin Kosinski, Przemyslaw Biecek, and Scheipl Fabian. 2018. *Survminer: Drawing Survival Curves Using "ggplot2"* (version 0.4.2). http://www.sthda.com/english/rpkgs/survminer/.

Koller, W., R. Pahwa, K. Busenbark, J. Hubble, S. Wilkinson, A. Lang, P. Tuite, et al. 1997. "High-Frequency Unilateral Thalamic Stimulation in the Treatment of Essential and Parkinsonian Tremor." *Annals of Neurology* 42 (3): 292–99.

Kong, Vincent, Gabriel A. Devenyi, Daniel Gallino, Gülebru Ayranci, Jürgen Germann, Colleen Rollins, and M. Mallar Chakravarty. 2018. "Early-in-Life Neuroanatomical and Behavioural Trajectories in a Triple Transgenic Model of Alzheimer's Disease." *Brain Structure & Function*, June. https://doi.org/10.1007/s00429-018-1691-4.

Kumar, R., A. Dagher, W. D. Hutchison, A. E. Lang, and A. M. Lozano. 1999. "Globus Pallidus Deep Brain Stimulation for Generalized Dystonia: Clinical and PET Investigation." *Neurology* 53: 871–74.

Lauterbur, P. C. 1973. "Image Formation by Induced Local Interactions: Examples Employing Nuclear Magnetic Resonance." *Nature* 242 (March): 190–91.

Laxton, Adrian W., David F. Tang-Wai, Mary Pat McAndrews, Dominik Zumsteg, Richard Wennberg, Ron Keren, John Wherrett, et al. 2010. "A Phase I Trial of Deep Brain Stimulation of Memory Circuits in Alzheimer's Disease." *Annals of Neurology* 68 (4): 521–34.

Leoutsakos, Jeannie-Marie S., Haijuan Yan, William S. Anderson, Wael F. Asaad, Gordon Baltuch, Anna Burke, M. Mallar Chakravarty, et al. 2018. "Deep Brain Stimulation Targeting the Fornix for Mild Alzheimer Dementia (the ADvance Trial): A Two Year Follow-up Including Results of Delayed Activation." *Journal of Alzheimer's Disease: JAD*, June. https://doi.org/10.3233/JAD-180121.

Lerch, Jason, Chris Hammill, Matthijs van Eede, and Daniel Cassel. 2016. *RMINC: Statistical Tools for Medical Imaging NetCDF (MINC) Files* (version 1.4.4.0). https://CRAN.R-project.org/package=RMINC.

Lin, Y. J., and A. P. Koretsky. 1997. "Manganese Ion Enhances T1-Weighted MRI during Brain Activation: An Approach to Direct Imaging of Brain Function." *Magnetic Resonance in Medicine: Official Journal of the Society of Magnetic Resonance in Medicine / Society of Magnetic Resonance in Medicine* 38 (3): 378–88.

Lozano, Andres M., Lisa Fosdick, M. Mallar Chakravarty, Jeannie-Marie Leoutsakos, Cynthia Munro, Esther Oh, Kristen E. Drake, et al. 2016. "A Phase II Study of Fornix Deep Brain Stimulation in Mild Alzheimer's Disease." *Journal of Alzheimer's Disease: JAD* 54 (2): 777–87.

Meidahl, Anders Christian, Gerd Tinkhauser, Damian Marc Herz, Hayriye Cagnan, Jean Debarros, and Peter Brown. 2017. "Adaptive Deep Brain Stimulation for Movement Disorders: The Long Road to Clinical Therapy." *Movement Disorders: Official Journal of the Movement Disorder Society* 32 (6): 810–19.

Mielke, Michelle M., Prashanthi Vemuri, and Walter A. Rocca. 2014. "Clinical Epidemiology of Alzheimer's Disease: Assessing Sex and Gender Differences." *Clinical Epidemiology* 6 (January): 37–48.

Mogilner, Alon Y., Alim-Louis Benabid, and Ali R. Rezai. 2001. "Brain Stimulation: Current Applications and Future Prospects." *Thalamus & Related Systems* 1: 255–67.

Mosconi, Lisa. 2005. “Brain Glucose Metabolism in the Early and Specific Diagnosis of Alzheimer’s Disease.” *European Journal of Nuclear Medicine and Molecular Imaging* 32 (4): 486–510.

Mullan, M., F. Crawford, K. Axelman, H. Houlden, L. Lilius, B. Winblad, and L. Lannfelt. 1992. “A Pathogenic Mutation for Probable Alzheimer’s Disease in the APP Gene at the N-Terminus of Beta-Amyloid.” *Nature Genetics* 1 (5): 345–47.

Oddo, Salvatore, Antonella Caccamo, Jason D. Shepherd, M. Paul Murphy, Todd E. Golde, Rakez Kayed, Raju Metherate, Mark P. Mattson, Yama Akbari, and Frank M. LaFerla. 2003. “Triple-Transgenic Model of Alzheimer’s Disease with Plaques and Tangles: Intracellular Abeta and Synaptic Dysfunction.” *Neuron* 39 (3): 409–21.

Perrin, Jennifer S., Pierre-Yves Hervé, Gabriel Leonard, Michel Perron, G. Bruce Pike, Alain Pitiot, Louis Richer, Suzanne Veillette, Zdenka Pausova, and Tomás Paus. 2008. “Growth of White Matter in the Adolescent Brain: Role of Testosterone and Androgen Receptor.” *The Journal of Neuroscience: The Official Journal of the Society for Neuroscience* 28 (38): 9519–24.

Pohodich, Amy E., Hari Yalamanchili, Ayush T. Raman, Ying-Wooi Wan, Michael Gundry, Shuang Hao, Haijing Jin, Jianrong Tang, Zhandong Liu, and Huda Y. Zoghbi. 2018. “Forniceal Deep Brain Stimulation Induces Gene Expression and Splicing Changes That Promote Neurogenesis and Plasticity.” *eLife* 7 (March). https://doi.org/10.7554/eLife.34031.

Ponce, Francisco A., Wael F. Asaad, Kelly D. Foote, William S. Anderson, G. Rees Cosgrove, Gordon H. Baltuch, Kara Beasley, et al. 2016. “Bilateral Deep Brain Stimulation of the Fornix for Alzheimer’s Disease: Surgical Safety in the ADvance Trial.” *Journal of Neurosurgery* 125 (1): 75–84.

Qiu, Lily R., Darren J. Fernandes, Kamila U. Szulc-Lerch, Jun Dazai, Brian J. Nieman, Daniel H. Turnbull, Jane A. Foster, Mark R. Palmert, and Jason P. Lerch. 2018. “Mouse MRI Shows Brain Areas Relatively Larger in Males Emerge before Those Larger in Females.” *Nature Communications* 9 (1). https://doi.org/10.1038/s41467-018-04921-2.

Qiu, Lily R., Jürgen Germann, Shoshana Spring, Christina Alm, Dulcie A. Vousden, Mark R. Palmert, and Jason P. Lerch. 2013. “Hippocampal Volumes Differ across the Mouse Estrous Cycle, Can Change within 24hours, and Associate with Cognitive Strategies.” *NeuroImage* 83 (December): 593–98.

R Core Team. 2016. *R: A Language and Environment for Statistical Computing* (version 3.2.4). http://www.R-project.org/.

Riudavets, Miguel A., Leonardo Bartoloni, Juan C. Troncoso, Olga Pletnikova, Peter St George-Hyslop, Marcelo Schultz, Gustavo Sevlever, and Ricardo F. Allegri. 2013. “Familial Dementia with Frontotemporal Features Associated with M146V Presenilin-1 Mutation.” *Brain Pathology* 23 (5): 595–600.

Rollins, Colleen, Daniel Gallino, Vincent Kong, Gülebru Ayranci, Gabriel A. Devenyi, Jürgen Germann, and Megha Mallar Chakravarty. n.d. “Contributions of a High-Fat Diet to Alzheimer’s Disease-Related Decline: A Longitudinal Behavioural and Structural Neuroimaging Study.” *Brain Structure & Function*.

Sankar, Tejas, M. Mallar Chakravarty, Agustin Bescos, Monica Lara, Toshiki Obuchi, Adrian W. Laxton, Mary Pat McAndrews, et al. 2015. “Deep Brain Stimulation Influences Brain Structure in Alzheimer’s Disease.” *Brain Stimulation* 8 (3): 645–54.

Sankar, Tejas, Nir Lipsman, and Andres M. Lozano. 2014. “Deep Brain Stimulation for

Disorders of Memory and Cognition." *Neurotherapeutics: The Journal of the American Society for Experimental NeuroTherapeutics* 11 (3): 527–34.
Sankar, Tejas, Stanley X. Li, Toshiki Obuchi, Alfonso Fasano, Melanie Cohn, Mojgan Hodaie, M. Mallar Chakravarty, and Andres M. Lozano. 2016. "Structural Brain Changes Following Subthalamic Nucleus Deep Brain Stimulation in Parkinson's Disease." *Movement Disorders: Official Journal of the Movement Disorder Society* 31 (9): 1423–25.
Sepúlveda, M. R., T. Dresselaers, P. Vangheluwe, W. Everaerts, U. Himmelreich, A. M. Mata, and F. Wuytack. 2012. "Evaluation of Manganese Uptake and Toxicity in Mouse Brain during Continuous MnCl2 Administration Using Osmotic Pumps: Mn2+ UPTAKE AND TOXICITY IN MOUSE BRAIN." *Contrast Media & Molecular Imaging* 7 (4): 426–34.
Stone, Scellig S. D., Cátia M. Teixeira, Loren M. Devito, Kirill Zaslavsky, Sheena A. Josselyn, Andres M. Lozano, and Paul W. Frankland. 2011. "Stimulation of Entorhinal Cortex Promotes Adult Neurogenesis and Facilitates Spatial Memory." *The Journal of Neuroscience: The Official Journal of the Society for Neuroscience* 31 (38): 13469–84.
Sundermann, Erin E., Anat Biegon, Leah H. Rubin, Richard B. Lipton, Wenzhu Mowrey, Susan Landau, Pauline M. Maki, and Alzheimer's Disease Neuroimaging Initiative. 2016. "Better Verbal Memory in Women than Men in MCI despite Similar Levels of Hippocampal Atrophy." *Neurology* 86 (15): 1368–76.
Tustison, Nicholas J., Brian B. Avants, Philip A. Cook, Yuanjie Zheng, Alexander Egan, Paul A. Yushkevich, and James C. Gee. 2010. "N4ITK: Improved N3 Bias Correction." *IEEE Transactions on Medical Imaging* 29 (6): 1310–20.
Van Hoesen, G. W., B. T. Hyman, and A. R. Damasio. 1991. "Entorhinal Cortex Pathology in Alzheimer's Disease." *Hippocampus* 1 (1): 1–8.
Vidailhet, Marie, Laurent Vercueil, Jean-Luc Houeto, Pierre Krystkowiak, Alim-Louis Benabid, Philippe Cornu, Christelle Lagrange, et al. 2005. "Bilateral Deep-Brain Stimulation of the Globus Pallidus in Primary Generalized Dystonia." *The New England Journal of Medicine* 352 (5): 459–67.
Vincent, Robert D., Peter Neelin, Najmeh Khalili-Mahani, Andrew L. Janke, Vladimir S. Fonov, Steven M. Robbins, Leila Baghdadi, et al. 2016. "MINC 2.0: A Flexible Format for Multi-Modal Images." *Frontiers in Neuroinformatics* 10 (August): 35.
Vorhees, Charles V., and Michael T. Williams. 2006. "Morris Water Maze: Procedures for Assessing Spatial and Related Forms of Learning and Memory." *Nature Protocols* 1 (2): 848–58.
Vousden, Dulcie A., Elizabeth Cox, Rylan Allemang-Grand, Christine Laliberté, Lily R. Qiu, Zsuzsa Lindenmaier, Brian J. Nieman, and Jason P. Lerch. 2018. "Continuous Manganese Delivery via Osmotic Pumps for Manganese-Enhanced Mouse MRI Does Not Impair Spatial Learning but Leads to Skin Ulceration." *NeuroImage* 173 (June): 411–20.
Williams, Michael T., Laronda L. Morford, Sandra L. Wood, Tanya L. Wallace, Masao Fukumura, Harry W. Broening, and Charles V. Vorhees. 2003. "Developmental D-Methamphetamine Treatment Selectively Induces Spatial Navigation Impairments in Reference Memory in the Morris Water Maze While Sparing Working Memory." *Synapse* 48 (3): 138–48.
Xia, Frances, Adelaide Yiu, Scellig S. D. Stone, Soojin Oh, Andres M. Lozano, Sheena A. Josselyn, and Paul W. Frankland. 2017. "Entorhinal Cortical Deep Brain Stimulation Rescues Memory Deficits in Both Young and Old Mice Genetically Engineered to Model Alzheimer's Disease." *Neuropsychopharmacology: Official Publication of the American*

*College of Neuropsychopharmacology* 42 (13): 2493–2503.
Zhang, Chao, Wen-Han Hu, De-Long Wu, Kai Zhang, and Jian-Guo Zhang. 2015. "Behavioral Effects of Deep Brain Stimulation of the Anterior Nucleus of Thalamus, Entorhinal Cortex and Fornix in a Rat Model of Alzheimer's Disease." *Chinese Medical Journal* 128 (9): 1190–95.

**Figure 1. Cox proportional hazard curves of latency-to-escape at a) 3 weeks post-stimulation and b) 6 weeks post-stimulation.** Percent of mice in each treatment group which have escaped the maze is displayed over the trial time, which is capped at 120 s. Groups are sham stimulated (sham), electrodeless controls (none) and stimulated (stim). Trial 1 is excluded due to mice being naive of new platform location. Each curve is enveloped by a lighter-coloured 95% confidence interval, and is marked with a dashed, black line at the time when half of mice of that group have found the platform. * significant at $\alpha = 0.05$ ($p < 0.0071$), ˙ trending at $\alpha = 0.10$ ($p < 0.014$)

**Figure 2. Cox proportional hazard curves of latency-to-escape at a) 3 weeks post-stimulation and b) 6 weeks post-stimulation broken down by sex.** Percent of mice in each treatment group which have escaped the maze is displayed over the trial time, which is capped at 120 s. Groups are sham stimulated females (sham, f), sham stimulated males (sham, m), stimulated females (stim, f) and stimulated males (stim, m). Trial 1 is excluded due to mice being naive of new platform location. Each curve is enveloped by a lighter-coloured 95% confidence interval, and is marked with a dashed, black line at the time when half of mice of that group have found the platform. * significant interaction term at $\alpha = 0.05$ ($p < 0.0071$)

**Figure 3. Mean latency to previous platform location on trial 1 (pseudo-probe trial).** Error bars represent standard error of the mean. Females are displayed on top and males on the bottom. Groups are sham stimulated (sham), electrodeless controls (none) and stimulated (stim). * $p < 0.05$ by non parametric Mann-Whitney *U* test.

**Figure 4. General volumetric effects of DBS-f by time point interaction as determined by voxel-based deformation analysis.** Peak voxel volumes of select areas are shown proportional to pre-stimulation baseline image. Each voxel of origin is indicated with a reticle on a coronal slice of the original t-statistic map. Stimulated animals displayed areas by the final time point

that were relatively larger (orange) or smaller (blue) than sham animals. T-statistic values are thresholded at a minimum FDR value of $q < 0.20$, and extend to their max value.

**Figure 5. Differential volumetric effects of sex of DBS by time point interaction as determined by voxel-based deformation analysis.** Peak voxel volumes of example areas (left) are shown proportional to pre-stimulation baseline image. Each voxel of origin is indicated with a reticle on a coronal slice of the original t-statistic map (right). Orange indicates areas in which stimulation induced larger final volumes than controls in females while lowering final volumes in males. Blue indicates areas in which stimulation induced larger final volumes than controls in males while lowering final volumes in females. T-statistic values are thresholded at a minimum FDR value of $q < 0.20$, and extend to their max value.

**Figure 6. Experiment timeline.** Ticks denote week denominations. Black squares indicate Morris water maze (MWM) testing days and white diamonds are MRI acquisitions.

**Figure 7. Electrode dimensions and placement in a coronal section perspective at bregma.** Electrodes were implanted bilaterally (±0.75 mm) at Bregma (0 mm anterior-posterior) to a depth of 3 mm.

Figure
Click here to download Figure: fig1_singlecol_colour.eps

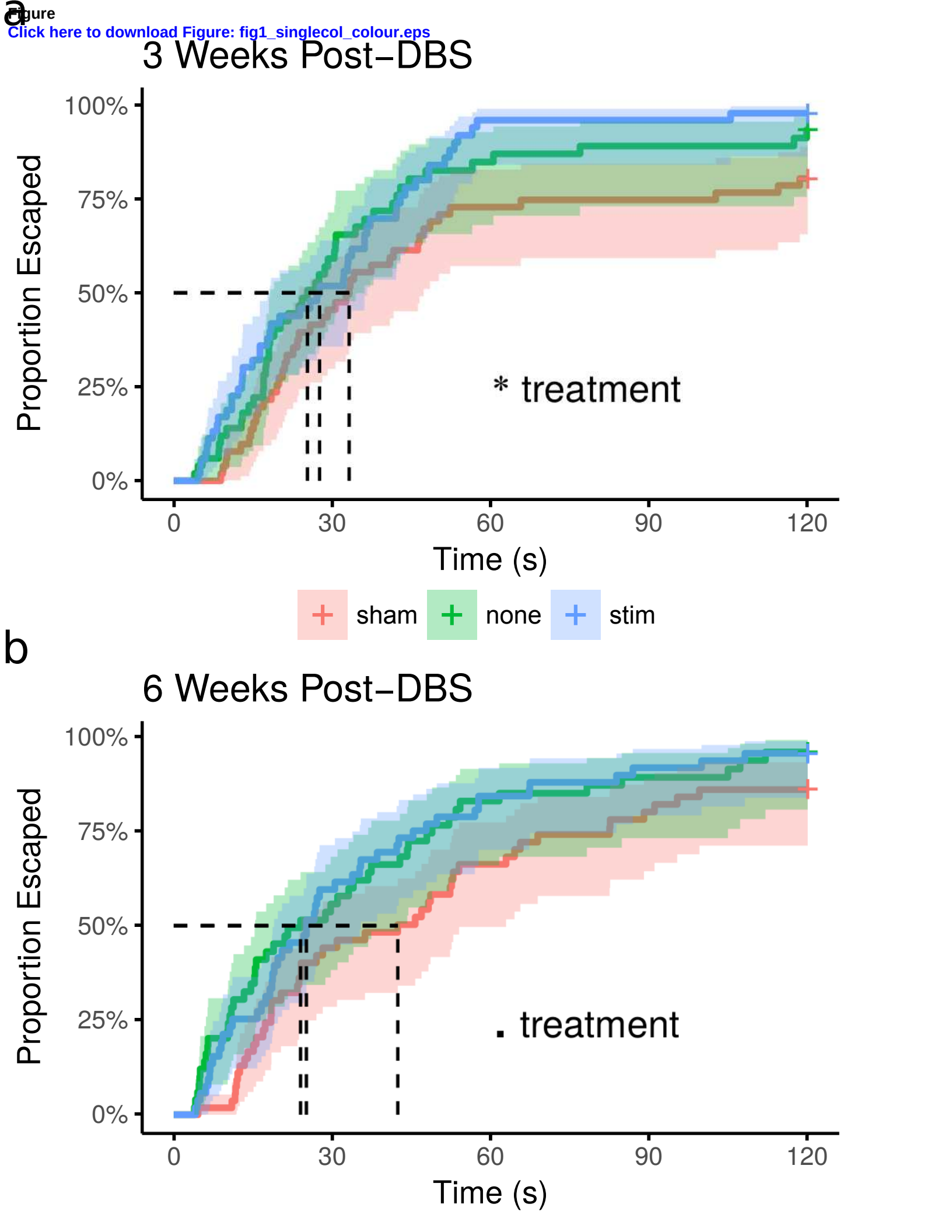

Figure
Click here to download Figure: fig2_singlecol_colour.eps

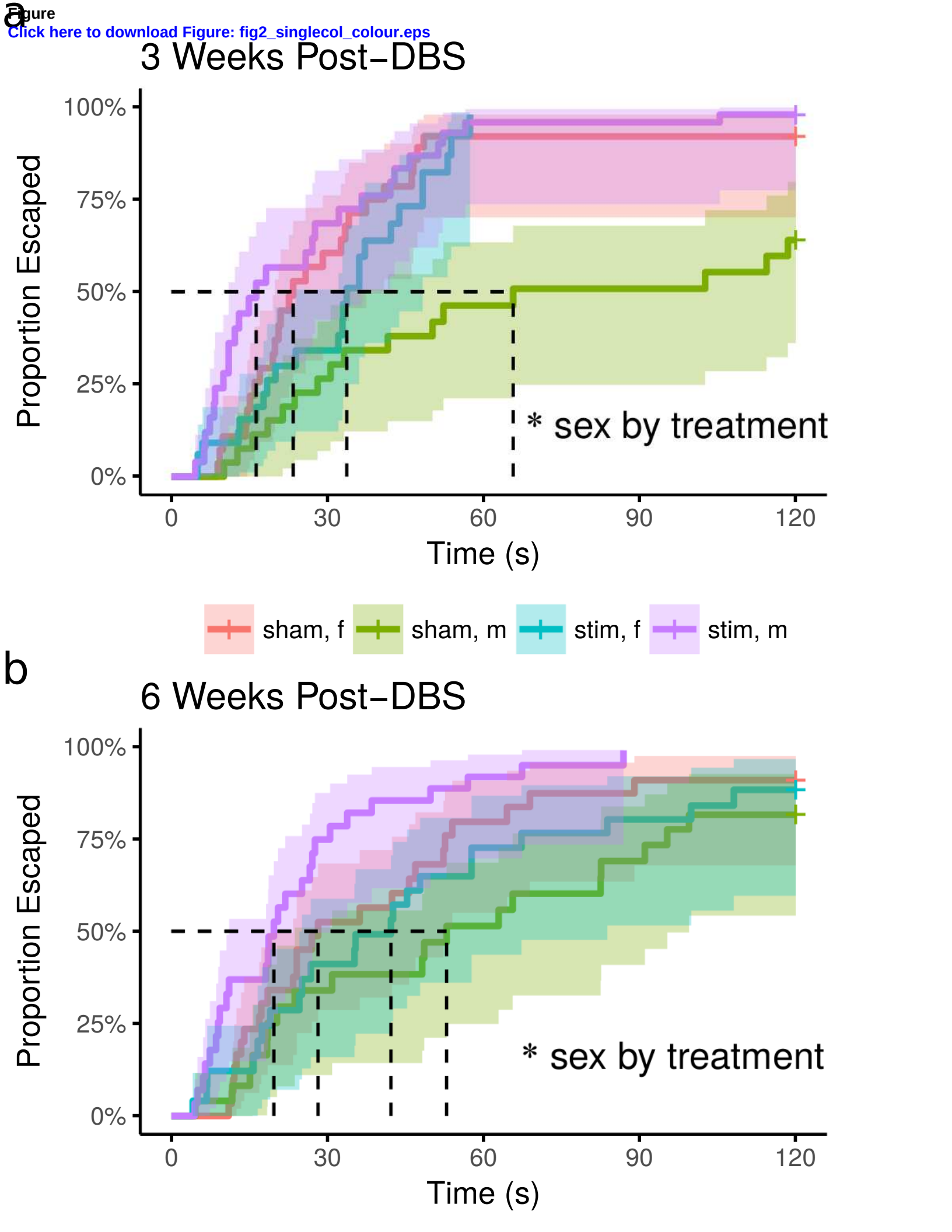

Figure

Click here to download Figure: fig3_1andhalfcol_colour.eps

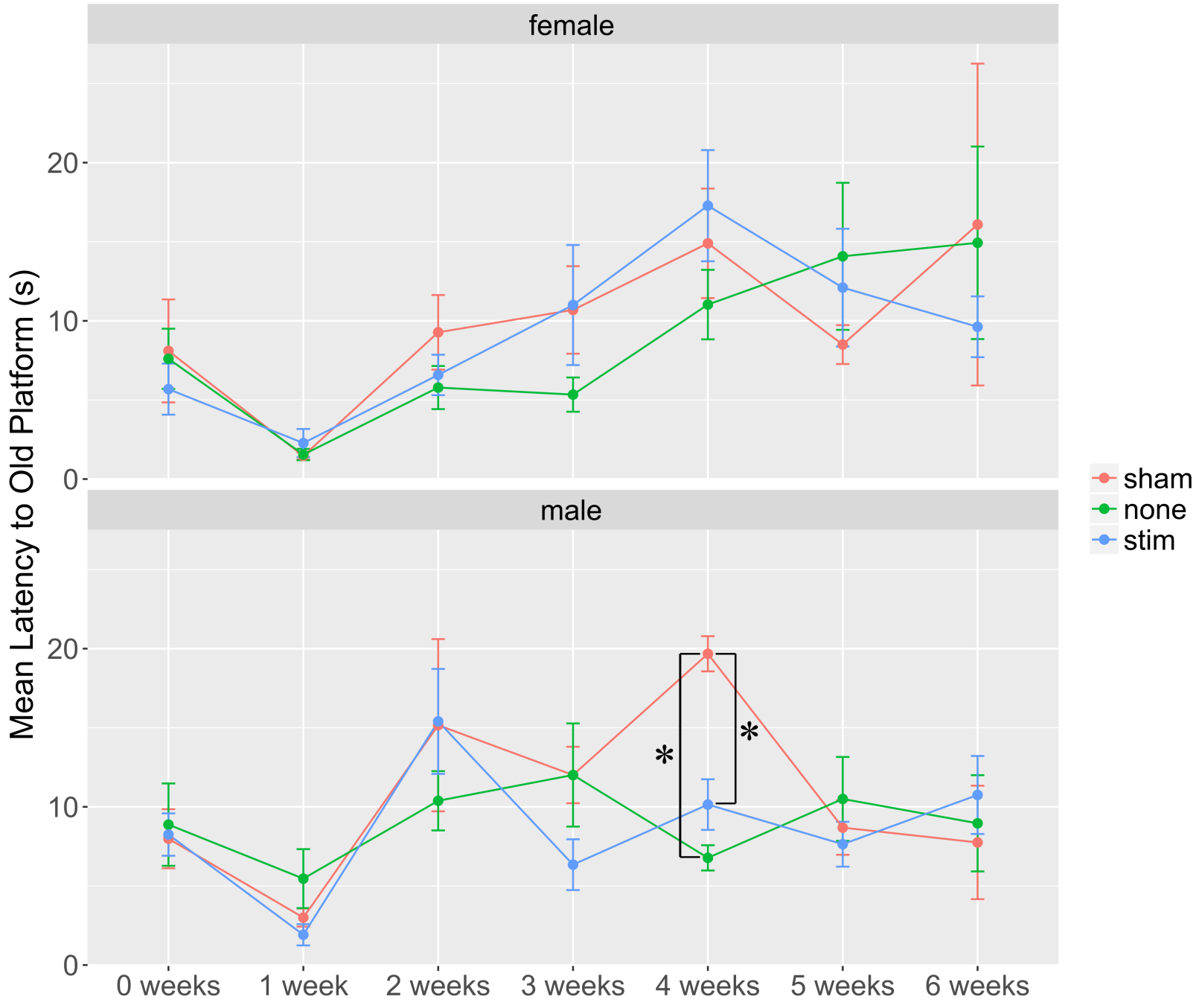

**Figure**

Click here to download Figure: fig4_fullpage_colour.eps

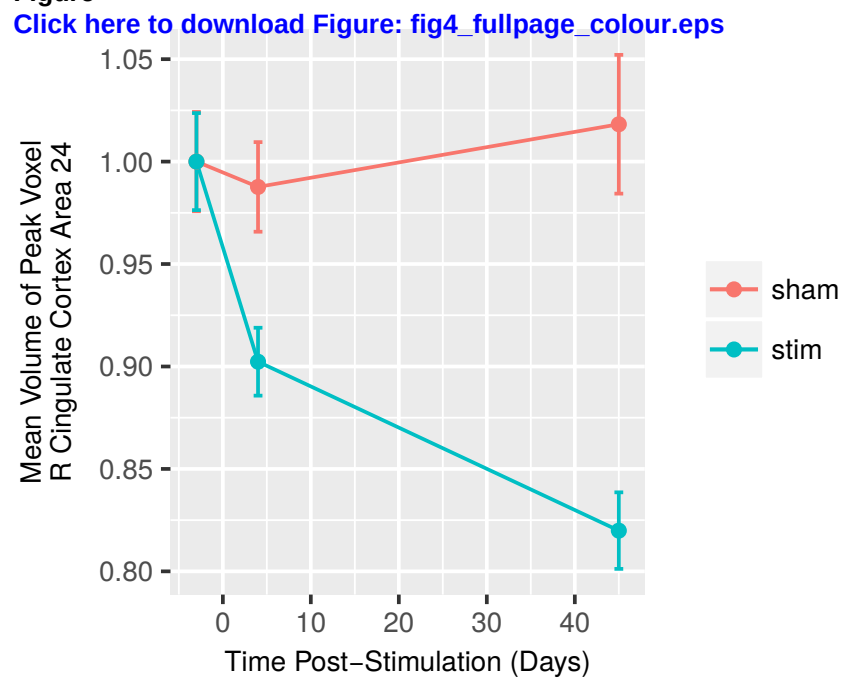


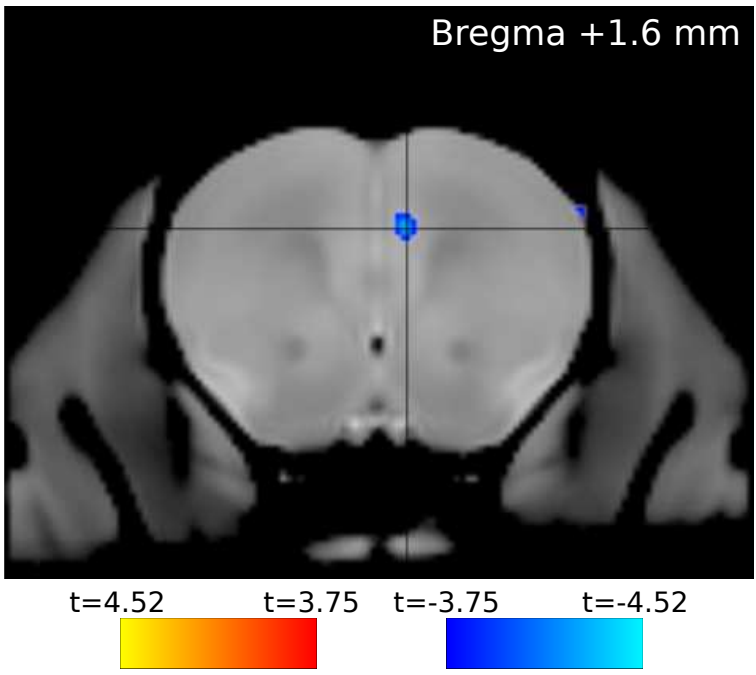


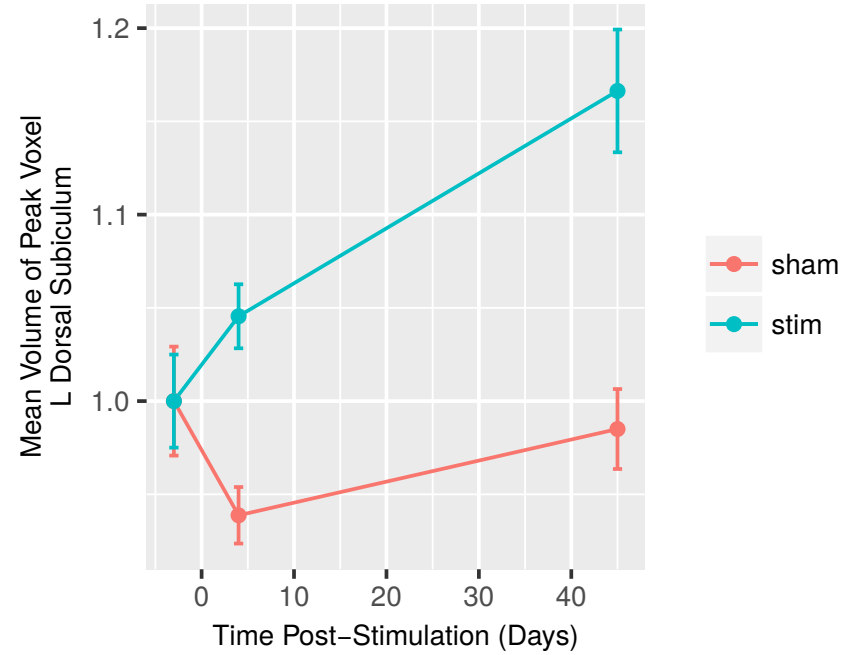


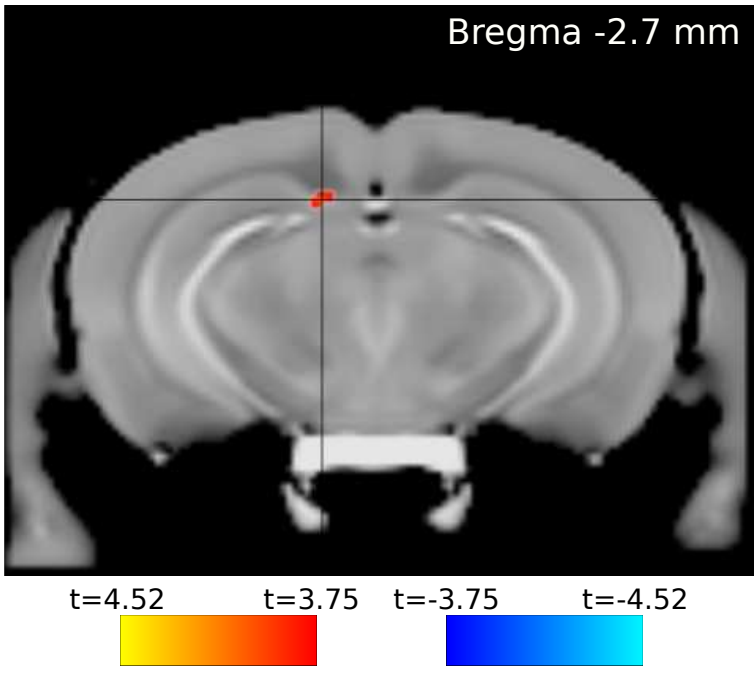


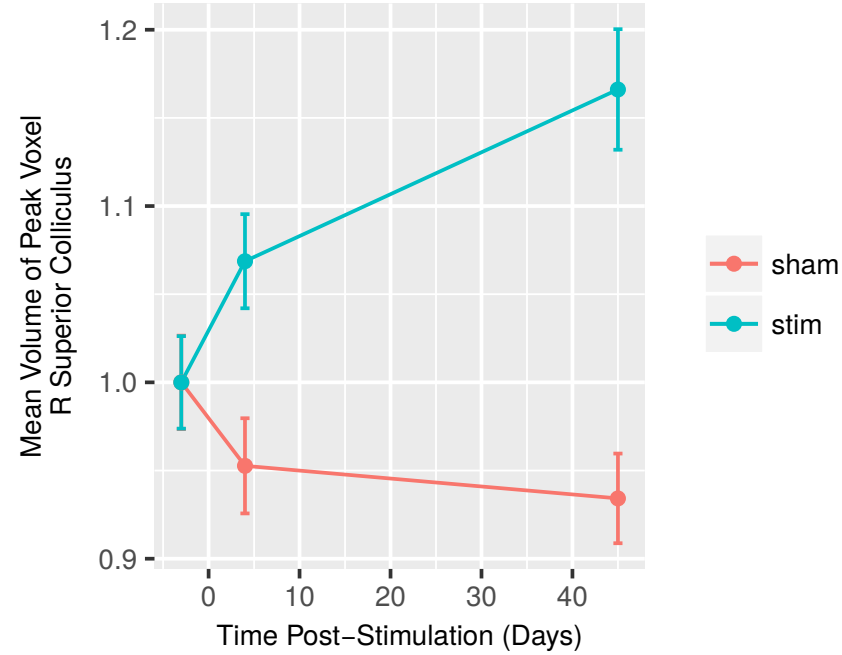


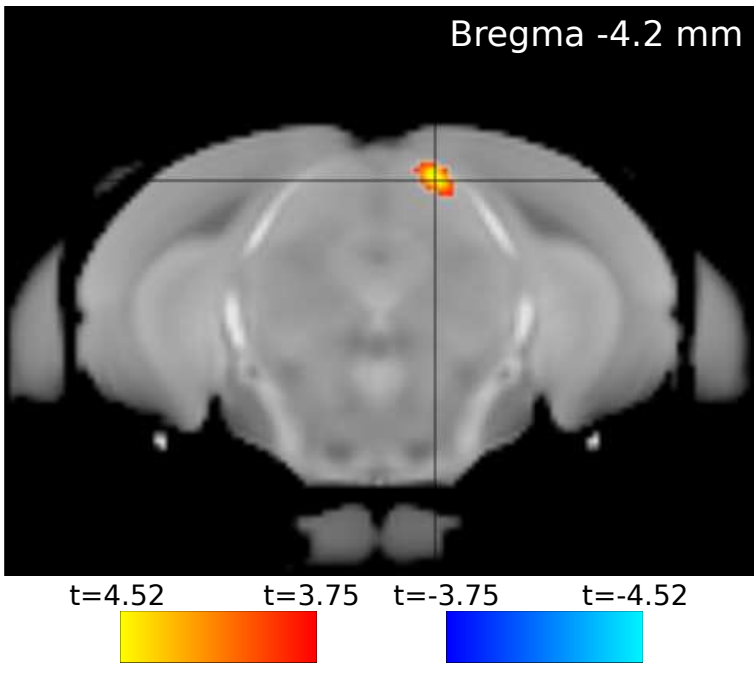

Figure

Click here to download Figure: fig5_fullpage_colour.eps

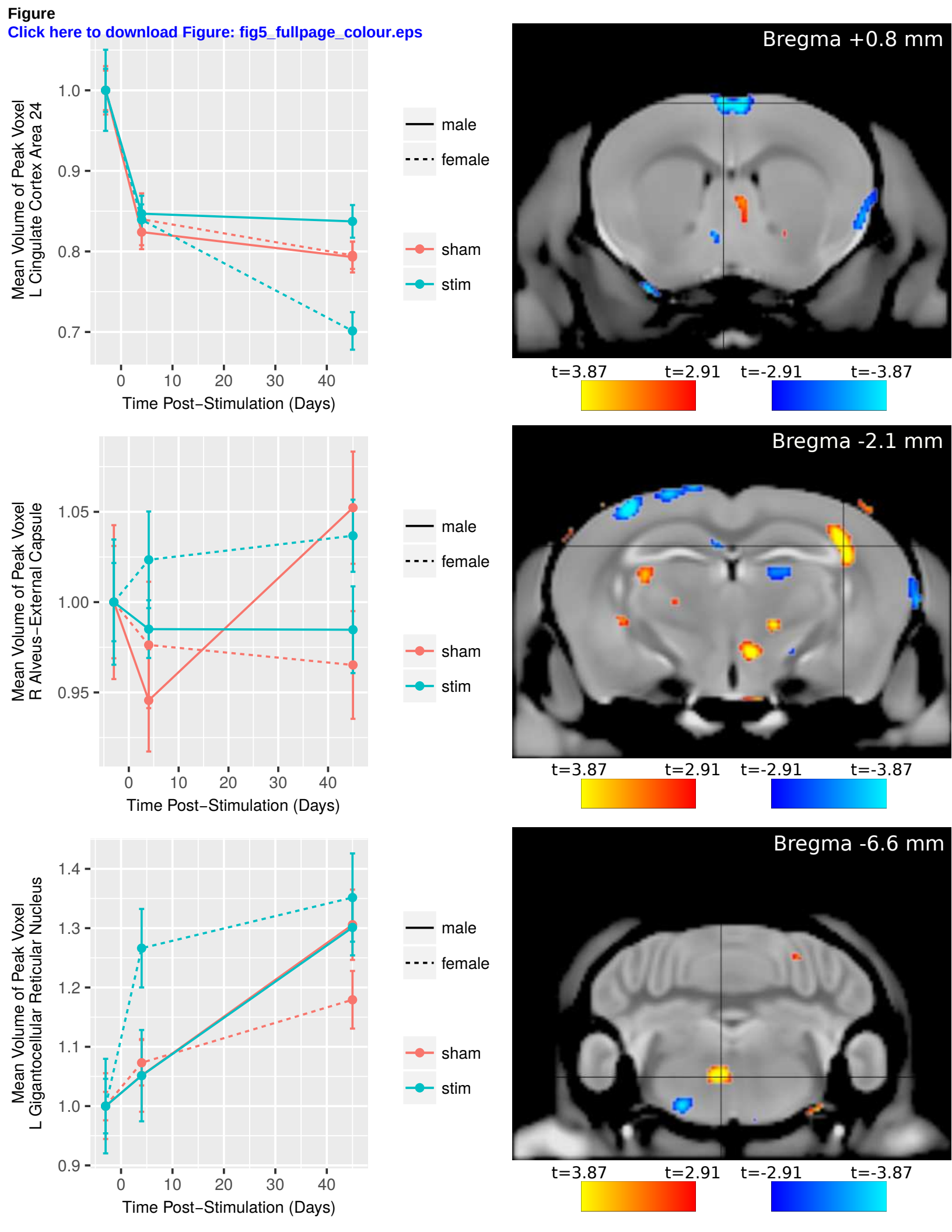

**Figure**

Click here to download Figure: fig6_1andhalfcol.eps

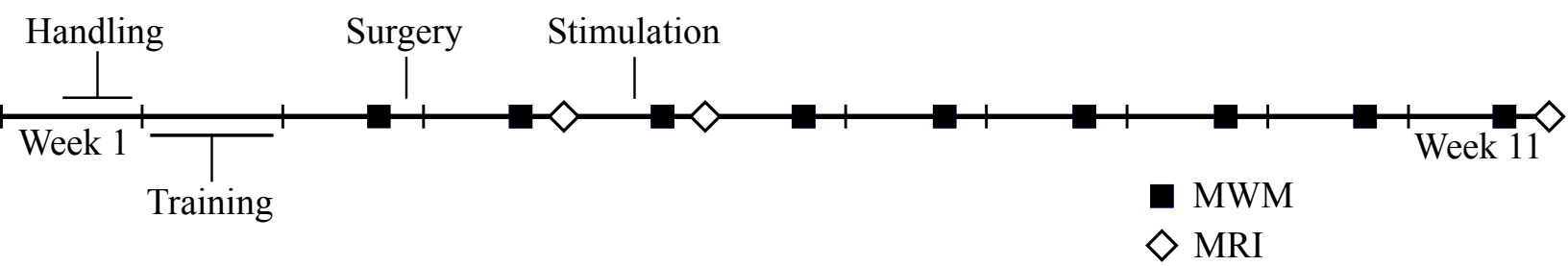

Figure
Click here to download Figure: fig7_singlecol.eps

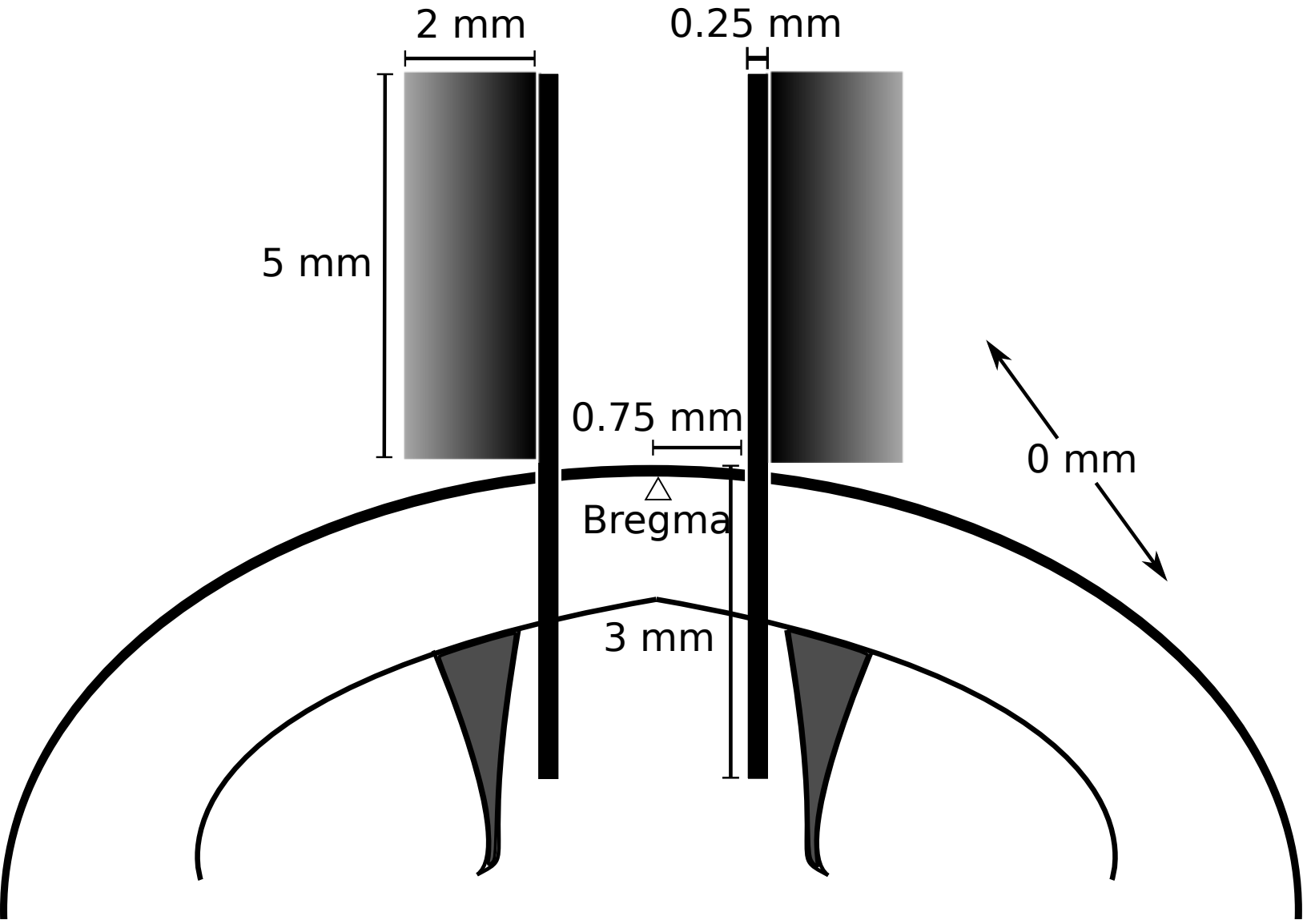

**Electronic Supplementary Material (online publication only)**

**Click here to download Electronic Supplementary Material (online publication only): Supplementary.pdf**